

An Automated Region-Of-Interest Segmentation for Optic Disc Extraction

Jasem Almotiri and Khaled Elleithy

Computer Science Department
University of Bridgeport
Bridgeport, CT 06604 USA

jalmotir@my.bridgeport.edu, elleithy@bridgeport.edu

Abdelrahman Elleithy

Computer Science Department
William Paterson University
Wayne, NJ 07470, USA
ElleithyA@wpunj.edu

Abstract—Optic disc segmentation in retinal fundus images plays a critical rule in diagnosing a variety of pathologies and abnormalities related to eye retina. Most of the abnormalities that are related to optic disc lead to structural changes in the inner and outer zones of optic disc. Optic disc segmentation on the level of whole retina image degrades the detection sensitivity for these zones. In this paper, we present an automated technique for the Region-Of-Interest segmentation of *optic disc* region in retinal images. Our segmentation technique reduces the processing area required for optic disc segmentation techniques leading to notable performance enhancement and reducing the amount of the required computational cost for each retinal image. DRIVE, DRISHTI-GS and DiaRetDB1 datasets were used to test and validate our proposed pre-processing technique.

Keywords—Region-Of-Interest; *optic disc*; *optic disc segmentation*; *retina*; *Hough transform*; *fuzzy c-means*.

I. INTRODUCTION

Retina fundus images are used by ophthalmologists in the diagnosis of eye-related diseases. The analysis stage of retina image that follow the image capturing is considered a corner stone in the overall diagnosis process. Retinal image analysis includes locating and extracting many retinal anatomical structures in a separate view which eases the diagnosis, gives more insight and thereby, enhances the diagnosis accuracy. Retinal vessels, Fovea, different types of lesions, optic disc shown in Figure 1 are typical examples of retinal anatomical structures that represent target objects for a broad range of segmentation techniques and algorithms [1-4].

All methods designed for retinal image analysis or other objects consist of three major stages; *Pre-Processing*, *Processing* and *Post-Processing*. Pre-processing stage is considered a preliminary one since it affects the quality of subsequent stages and affects the overall segmentation performance [5]. This stage includes one or more of the operations; noise/artifacts removal, green, or red layer extraction, image contrast enhancement, and Region-Of-Interest (ROI) extraction. However, some methods used to reduce high dimensional data in the pre-processing [6].

An automated ROI detection module was proposed by Zhang *et al.* [7] using an image pre-processing step called *fringe removal*. The authors observed that the unbalanced brightness

found in the fringe of the optic disc rim goes behind failure in

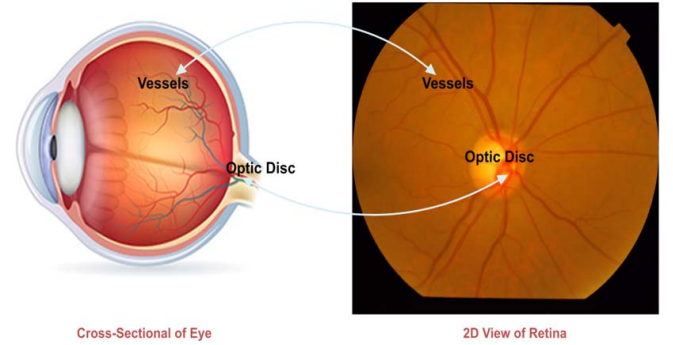


Figure 1. Retinal vessels and optic disc anatomical structures.

the optic disc.

Dehghani *et al.* [8] used the average of the histogram to localize the optic disc regions while other researchers exploited the elliptic shape of the optic disc and wavelet transform for performing this task as in [9]. Average filtering process followed by thresholding was used by [10] whereas, an iterative thresholding process followed by connected component analysis was used by [11] for optic disc center localization as a pre-step before optic disc contour localization.

Instead of letting the user to manually choose the optic disc region, this paper presents an intelligent automated ROI localization, and extraction technique based on fuzzy c-means and Hough transform. The rest of this paper is organized as follows. Section II presents the proposed region-of-interest extraction scheme. Section III presents experimental results, and Section IV concludes the paper.

II. PROPOSED METHOD

In this work, we propose a new technique that combines two techniques; Fuzzy c-means and Hough transform. Fuzzy c-means associated with morphological operations was used as an edge-map creator whereas Hough transform was utilized for the optic disc center localization. Morphological operations played more than a complement step; namely, it plays a central role in case of extracting the optic disc ROI in pathological fundus images. The general flowchart of the proposed technique is

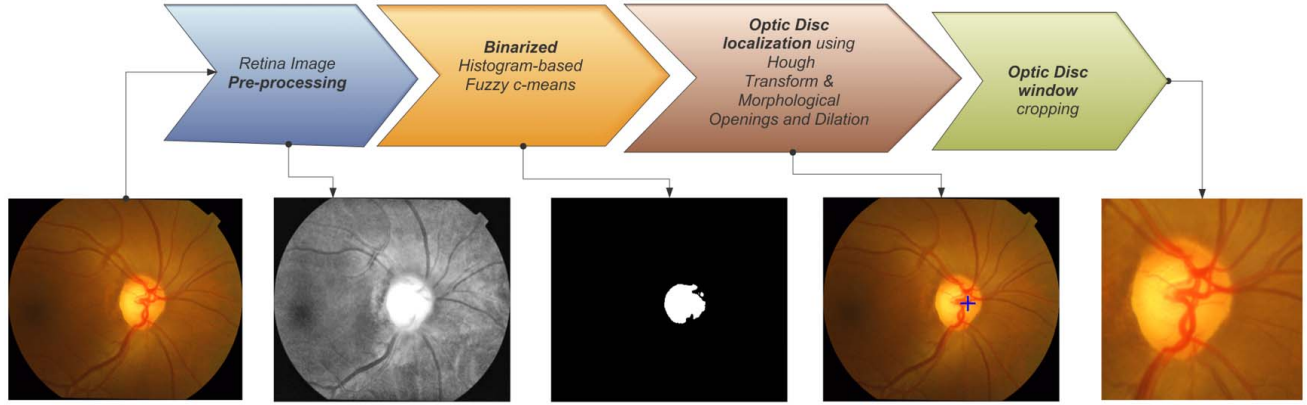


Figure 2. Major stages of optic disc ROI extraction technique.

illustrated in Figure 2.

Our identification technique is composed of the following four major stages: (1) Retinal image pre-processing. (2) Fuzzy c-means binarization. (3) Optic disc localization. (4) Optic disc cropping.

A. Retinal Image Pre-processing

Optic disc region normally exhibits a high contrast in comparison to other anatomical structures in digital fundus images. However, the existence of large vessels passing through the optic disc region besides possible neighbor lesions makes the image contrast enhancement a very first step. Since the contrast of the optic disc in the red channel layer is better in comparison to blue and green layers of RGB color fundus

image; we extracted the red layer of raw retina image then the successive steps of pre-processing were applied on it as shown in Figure 3.a. In the second step of the pre-processing stage, a Contrast Limited Adaptive Histogram Equalization (CLAHE) followed by a median filtering of 9×9 sized-window were applied on the gray scale image found in first step of this stage, as illustrated in Figure 3.b and 3.c.

B. Fuzzy c-means Binarization

Optic disc appears as circular or semi-elliptical spot on the surface of retina. Once the optic disc has been localized; ROI extraction proceeds smoothly. Thus, we utilized Hough transform to localize the center of the optic disc circle. However, Since Hough transform was originally designed for lines and parametric curves detection, edge detection is often

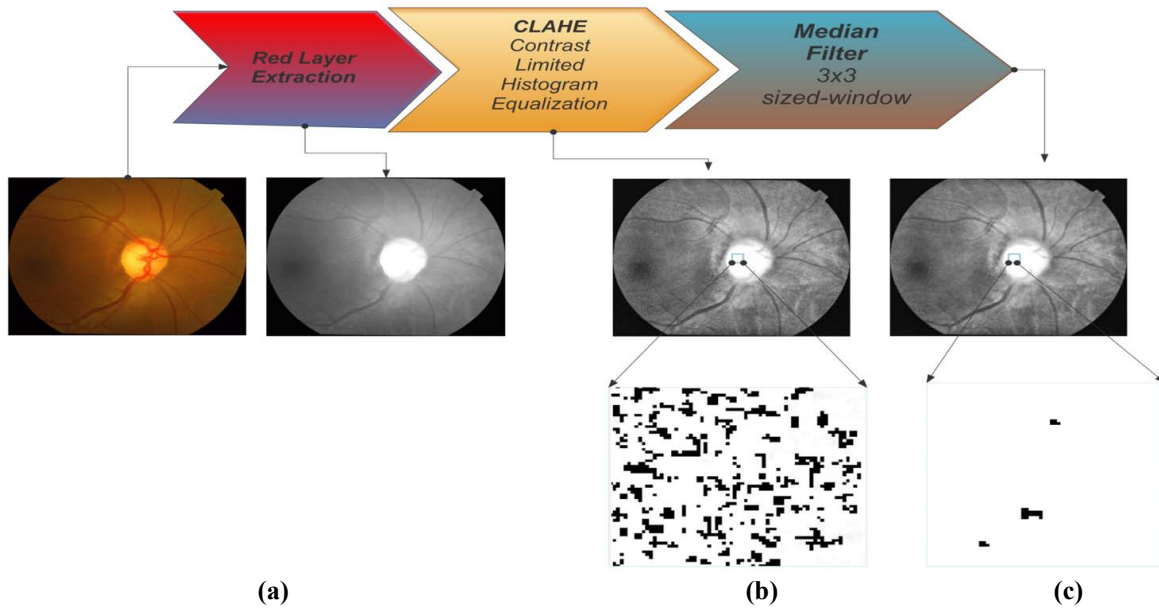


Figure 3. Pre-processing steps: (a) Red layer output. (b) CLAHE output. (c) Median filter output.

used as pre-processing step to Hough transform. Therefore, we use fuzzy c-means [12] for the sake of edge-map detection. Using $c = 25$, the pre-processed image was clustered into 25 clusters (image of 25 gray levels. The number of clusters was chosen, in such a way that one cluster (of high gray level = c) corresponds to the optic disc region or at least part of it, and the other corresponds to the other background objects as illustrated in Figure 4.b The output of fuzzy c-means algorithm is binarized as in (1):

$$I_{FCM}^B = \begin{cases} 1; & \text{if } I_{FCM} = c \\ 0, & \text{otherwise.} \end{cases} \quad (1)$$

Where I_{FCM}^B is the binarized version of fuzzy c-means output I_{FCM} .

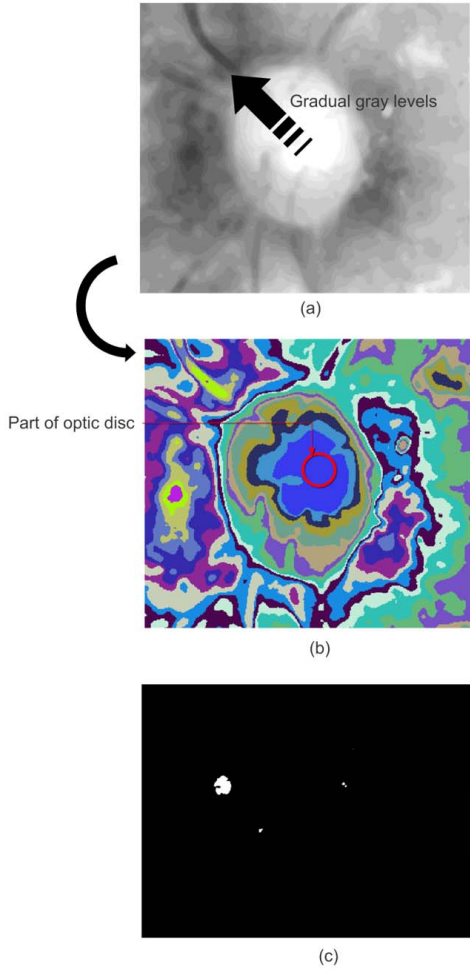


Figure 4. Fuzzy c-means output of a pathological retina image. (a) Actual fuzzy c-means output of $c = 25$ clusters yields 25 gray levels gradually decrease as we move away of the optic disc center. (b) color-substituted image corresponds to image in (a) for more gray levels clarification. (c) Binarized version of fuzzy c-means output where it shows a part of optic disc center (large white spot), and other small spots represents exudates lesions in this image.

C. Optic Disc Localization

In order for Hough transform to work, it requires an edge-map image. Moreover, the binarized image of the fuzzy c-means binarization may contain residual white spots corresponding to fundus camera artifacts, noise or as often due to neighbor retina lesions such as hard and soft exudates lesions. Therefore, as a pre-processing step before using Hough transform for optic disc center localization, we carried out a set of successive morphological operations in order to remove these artifacts and create the edge-map image. Morphological opening followed by dilation removes the objects (of size less than or equals 1500 pixels). Then, the boundary pixels (edge-map) of clean region is established as elaborated in Figure 5. (b), (c) and (d).

D. Optic Disc Cropping

Since Hough transform detects the coordinates (x_{center}, y_{center}) of the optic disc circle as shown in Figure 5. (e), a perfect circle can be synthesized with a radius r . Choosing the radius value depends on the validation dataset used; because each dataset produced using fundus camera with particular specifications in terms of image size and pixel resolution. Radius value r was used in our technique to establish the widows' borders of the optic disc region as in (2):

$$\begin{pmatrix} window_{width}=2*r \\ window_{length}=2*r \end{pmatrix} \quad (2)$$

Then, using dimensions specified in (2) and MATLAB ® image cropping function, the final optic disc ROI has been extracted as shown in Figure 5. (f).

III. EXPERIMENTAL RESULTS AND DISCUSSION

This section explores and discusses the experimental results obtained as a result of running our proposed optic disc ROI extraction system. The proposed system was developed and tested in the environment of MATLAB 2017a using image processing toolbox, using a personal laptop configured with Windows 10 professional with Intel Core i7 4Due 2.4,1.8GHZ CPU and 8.0 GB RAM.

In this section, the success of our proposed system in identifying and extracting the optic disc region in a non-pathological retina images was evaluated using public DRISHTI-GS dataset [13], which contains retinal fundus images for 50 patients using a 30 degrees field of view (FOV) at a resolution of 2896 x 1944 pixels. Figure 6 shows typical examples of optic disc localization and ROI extraction results of our proposed technique applied on DRISHTI-GS dataset where r is 400 pixels.

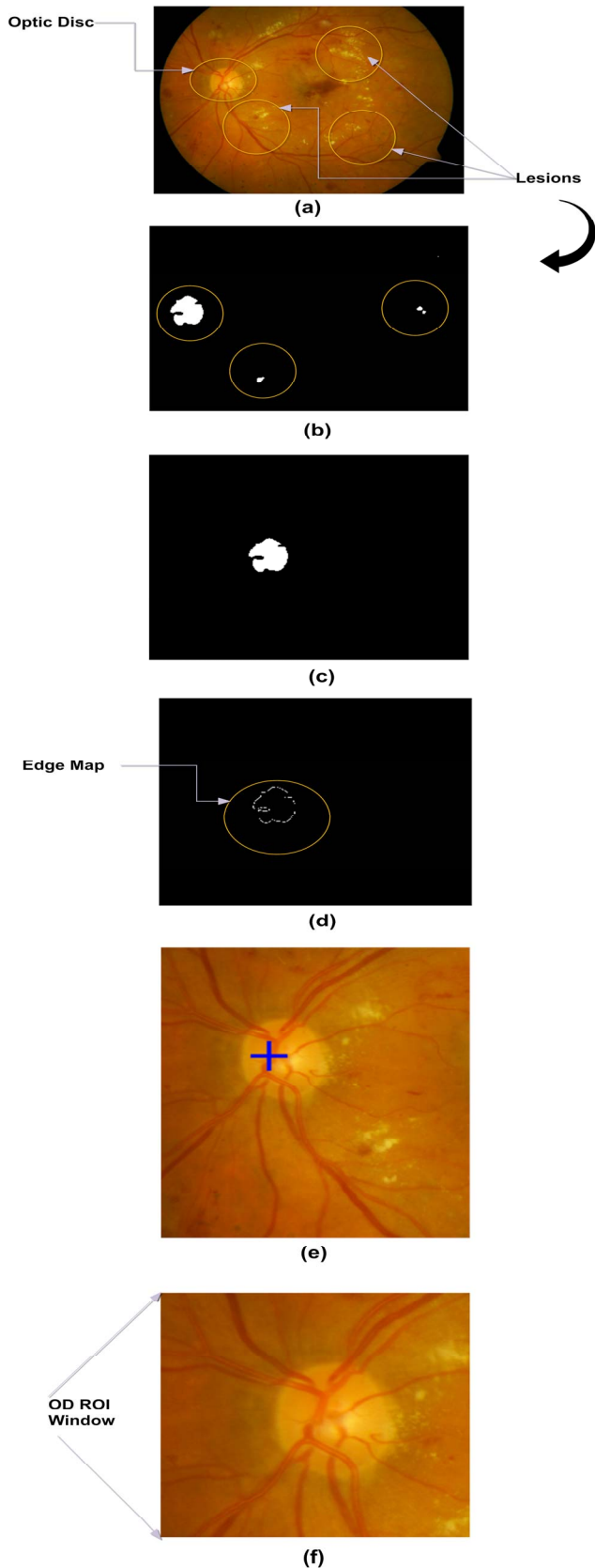


Figure 5. Optic disc localization and cropping: (a) abnormal (pathological) fundus image. (b) Fuzzy c-means binarization output. (c) Morphological cleaning. (d) Edge-map detection. (e) Optic disc center localization. (f) Optic disc ROI window.

As can be noted from Figure 6, the proposed technique is able to localize and extract the ROI successfully with the presence of camera artifacts and noise. This is due to applying fuzzy c-means as an edge-map tool for Hough transform rather than directly using a thresholding technique.

For pathological fundus images, we have validated our technique via DiaRetDB1 [14] dataset at the image level. This dataset consists of 89 color fundus images taken in Kuopio University Hospital of diabetic retinopathy abnormalities. Other images are normal, according to four experts involved in the diagnostic process. Figure 7 illustrates typical examples of the optic disc localization as well as the corresponding ROI extraction results of our proposed technique based on the pathological DiaRetDB1 dataset. As shown in Figure 7, the proposed technique is able to detect the optic disc region in pathological fundus images due to high clustering capability of the fuzzy c-means without the need for texture analysis.

For the sake of results comparison, an optic disc localization matched up to 96% of cases was reported by [7] segmentation results using ORIGA dataset [15], where the rest of images (remaining of 4%) have bad quality. In these cases, the user need to adjust OD ROI manually. However, our proposed technique showed better results in terms of localization and OD ROI segmentation where OD localization reached up to 100% for normal (and semi-normal) retina fundus images based on both DRISHTI-GS and DRIVE datasets whereas it has achieved 78.38% for subset of 37 pathological fundus images chosen from DiaRetDB1 dataset.

These results support the validity of our ROI segmentation technique and show that our technique gives exceptional results for both low and high noisy and pathological areas.

IV. CONCLUSION

One of the challenging issues with different types of segmentation tasks applied on retinal images is that the quality of acquired images is usually not good. This is due to noise or camera artifacts including uneven illumination, blurred and noisy regions as well as different types of retina pathologies. It is of considerable importance to enhance the quality of colored retinal images for reliable detection or segmentation. In this paper, an ROI extraction pre-processing technique was proposed for different types of retinal image segmentation. It was validated on both normal and abnormal retina images where it showed supreme performance in comparison to other optic disc ROI extraction techniques.

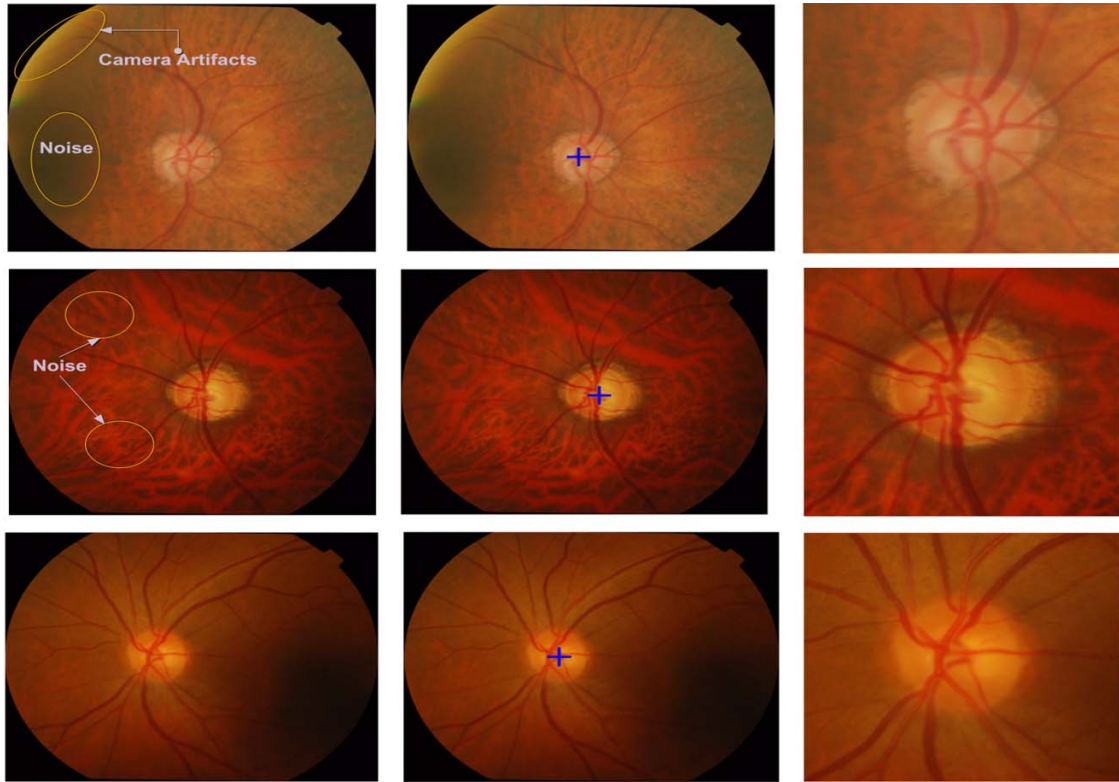


Figure 6. Optic disc localization and ROI segmentation results for the DRISHTI-DS dataset: Column 1: Original retinal images. Column 2: OD localization Column 3: Corresponding OD region of interest.

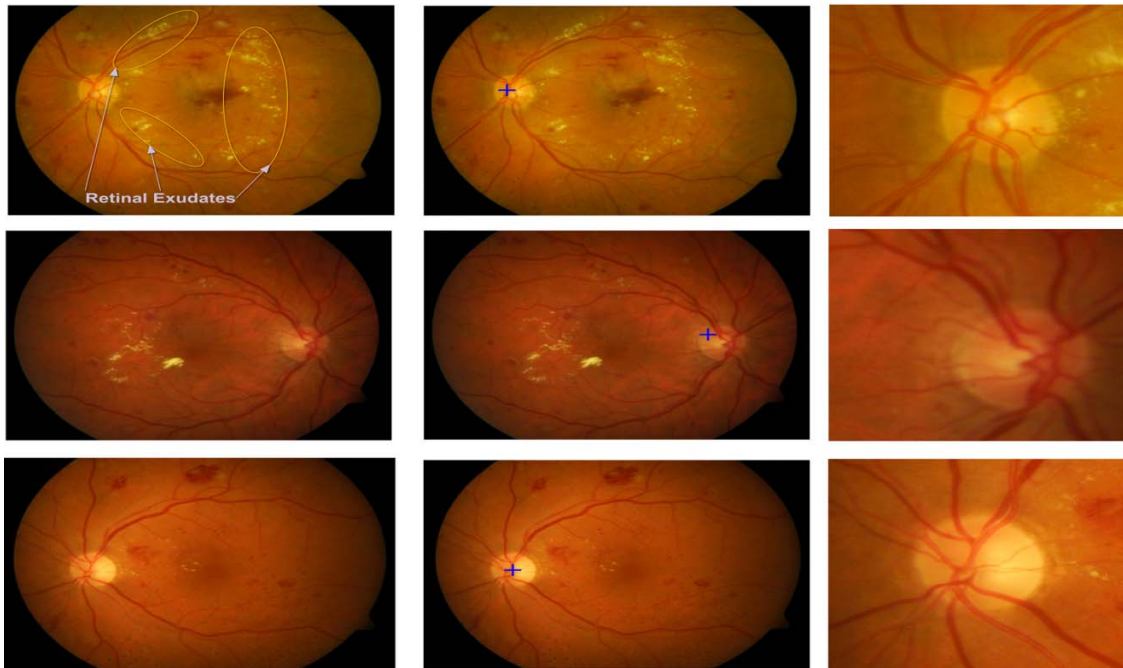


Figure 7. Optic disc localization and ROI segmentation results for the pathological DiaRetDB1 dataset. Column 1: Original retinal images. Column 2: OD localization Column 3: Corresponding OD region of interest.

REFERENCES

- [1] J. Almotiri, K. Elleithy, and A. Elleithy, "Retinal Vessels Segmentation Techniques and Algorithms: A Survey," *Applied Sciences*, vol. 8, p. 155, 2018.
- [2] C. L. Srinidhi, P. Aparna, and J. Rajan, "Recent advancements in retinal vessel segmentation," *Journal of medical systems*, vol. 41, p. 70, 2017.
- [3] A. Almazroa, R. Burman, K. Raahemifar, and V. Lakshminarayanan, "Optic disc and optic cup segmentation methodologies for glaucoma image detection: a survey," *Journal of ophthalmology*, vol. 2015, 2015.
- [4] M. M. Fraz, P. Remagnino, A. Hoppe, B. Uyyanonvara, A. R. Rudnicka, C. G. Owen, *et al.*, "Blood vessel segmentation methodologies in retinal images—a survey," *Computer methods and programs in biomedicine*, vol. 108, pp. 407-433, 2012.
- [5] M. Daneshzand, R. A. Zoroofi, and M. Faezipour, "MR image assisted drug delivery in respiratory tract and trachea tissues based on an enhanced level set method," in *Proceedings of the 2014 Zone 1 Conference of the American Society for Engineering Education*, 2014, pp. 1-7.
- [6] J. Almotiri, K. Elleithy, and A. Elleithy, "Comparison of autoencoder and Principal Component Analysis followed by neural network for e-learning using handwritten recognition," in *2017 IEEE Long Island Systems, Applications and Technology Conference (LISAT)*, 2017, pp. 1-5.
- [7] Z. Zhang, B. H. Lee, J. Liu, D. W. K. Wong, N. M. Tan, J. H. Lim, *et al.*, "Optic disc region of interest localization in fundus image for glaucoma detection in ARGALI," in *Industrial Electronics and Applications (ICIEA), 2010 the 5th IEEE Conference on*, 2010, pp. 1686-1689.
- [8] A. Dehghani, H. A. Moghaddam, and M.-S. Moin, "Optic disc localization in retinal images using histogram matching," *EURASIP Journal on Image and Video Processing*, vol. 2012, p. 19, 2012.
- [9] P. Pallawala, W. Hsu, M. L. Lee, and K.-G. A. Eong, "Automated optic disc localization and contour detection using ellipse fitting and wavelet transform," in *European conference on computer vision*, 2004, pp. 139-151.
- [10] M. U. Akram, A. Khan, K. Iqbal, and W. H. Butt, "Retinal images: optic disk localization and detection," in *International Conference Image Analysis and Recognition*, 2010, pp. 40-49.
- [11] P. Siddalingaswamy and K. G. Prabhu, "Automatic localization and boundary detection of optic disc using implicit active contours," *International Journal of Computer Applications*, vol. 1, pp. 1-5, 2010.
- [12] J. C. Bezdek, R. Ehrlich, and W. Full, "FCM: The fuzzy c-means clustering algorithm," *Computers & Geosciences*, vol. 10, pp. 191-203, 1984.
- [13] J. Sivaswamy, S. Krishnadas, G. D. Joshi, M. Jain, and A. U. S. Tabish, "Drishti-gs: Retinal image dataset for optic nerve head (onh) segmentation," in *Biomedical Imaging (ISBI), 2014 IEEE 11th International Symposium on*, 2014, pp. 53-56.
- [14] T. Kauppi, V. Kalesnykiene, J.-K. Kamarainen, L. Lensu, I. Sorri, A. Raninen, *et al.*, "The DIARETDB1 Diabetic Retinopathy Database and Evaluation Protocol," in *BMVC*, 2007, pp. 1-10.
- [15] Z. Zhang, F. S. Yin, J. Liu, W. K. Wong, N. M. Tan, B. H. Lee, *et al.*, "Origa-light: An online retinal fundus image database for glaucoma analysis and research," in *Engineering in Medicine and Biology Society (EMBC), 2010 Annual International Conference of the IEEE*, 2010, pp. 3065-3068.